



UNIVERSITY OF LEEDS

This is a repository copy of *Analysis of the physical properties of developing cotton fibres*.

White Rose Research Online URL for this paper:

<http://eprints.whiterose.ac.uk/81245/>

Version: Accepted Version

Article:

Kljun, A, El-Dessouky, HM, Benians, TAS et al. (4 more authors) (2014) Analysis of the physical properties of developing cotton fibres. *European Polymer Journal*, 51. 57 - 68. ISSN 0014-3057

<https://doi.org/10.1016/j.eurpolymj.2013.11.016>

Reuse

Unless indicated otherwise, fulltext items are protected by copyright with all rights reserved. The copyright exception in section 29 of the Copyright, Designs and Patents Act 1988 allows the making of a single copy solely for the purpose of non-commercial research or private study within the limits of fair dealing. The publisher or other rights-holder may allow further reproduction and re-use of this version - refer to the White Rose Research Online record for this item. Where records identify the publisher as the copyright holder, users can verify any specific terms of use on the publisher's website.

Takedown

If you consider content in White Rose Research Online to be in breach of UK law, please notify us by emailing eprints@whiterose.ac.uk including the URL of the record and the reason for the withdrawal request.



eprints@whiterose.ac.uk
<https://eprints.whiterose.ac.uk/>

Analysis of the physical properties of developing cotton fibres

Alenka Kljun,^a Hassan M. El-Dessouky,^{a,b} Thomas A. S. Benians,^c Florence Goubet,^d Frank Meulewaeter,^d J. Paul Knox,^c Richard S. Blackburn^{a,*}

^a Centre for Technical Textiles, University of Leeds, Leeds, LS2 9JT, UK; ^b Department of Physics, Faculty of Science, Mansoura University, Egypt; ^c Centre for Plant Sciences, University of Leeds, Leeds, LS2 9JT, UK; ^d Bayer CropScience NV, Technologiepark 38, 9000 Gent, Belgium

*Corresponding author: Tel.: +44 113 343 3757; Fax: +44 113 343 3704; e-mail: r.s.blackburn@leeds.ac.uk (R.S. Blackburn)

Abstract

Cotton fibres develop over four stages: initiation, elongation, secondary-wall thickening, and maturation. They develop a significant crystalline structure during the secondary wall thickening stage of development. Cotton fibres were harvested from 17 days to 60 days after flowering (dpa). Transmission Electron Microscopy (TEM), Interferometry, Attenuated Total Reflectance Fourier-transform Infrared (ATR-FTIR) spectroscopy, immunofluorescence labelling, and fluorescence spectroscopy were used to characterise the cotton fibres in different stages. It was found that, secondary wall thickening and micronaire remain fairly constant from 17 to 24 dpa, after that time significant change occurs until maturity. Maturity ratio increases as the fibres develop. Birefringence increases rapidly from 17 dpa to 26 dpa, then levels off up to 60 dpa. It is evident by comparing the Lateral Order Index (LOI) and

results from the binding of a crystalline-cellulose binding probe (CBM3a) that there is a significant increase in the degree of cellulose crystallinity from 17 dpa to 26 dpa. Hydrogen Bond Intensity (HBI) increased to 24 dpa and decreased from 24 to 40 dpa indicating significant changes in inter-molecular hydrogen bonds. From 40 to 60 dpa an increase of HBI was observed. It is concluded that during the maturation stage of cotton fibre development, water loss from lumen allows the cellulose chains to come closer together and to form intermolecular hydrogen-bonds. TEM, Interferometry, ATR-FTIR spectroscopy, and immunofluorescence labelling combined with fluorescence spectroscopy, were demonstrated to be useful techniques in quantifying physical changes in cotton fibres during development, offering advantages over traditional analytical techniques.

Keywords: cotton fibres; maturity; birefringence; ATR-FTIR; crystallinity.

1. Introduction

Cotton is the purest form of cellulose found in nature and cotton fibres have considerable economic significance. Therefore a fundamental understanding of cotton fibre structure and properties is important. Studies on the development of cotton fibre have concentrated on biochemical and cell structures from genetic and environmental perspectives [1].

Cotton fibres develop over four stages: (i) initiation; (ii) elongation; (iii) secondary-wall thickening; and (iv) maturation. Fibre initiation begins during flowering and fibres arise from the epidermal cells on the ovule surface [2,3]; the days after flowering are referred to as days post anthesis (dpa). Fibre elongation begins on the day of flowering by spherical expansion above the ovular surface and continues with primary cell wall deposition for 20 to 25 days

until reaching final fibre lengths of 22 to 35 mm. Secondary cell wall synthesis begins around 15 to 22 dpa and continues for 30 to 40 days. Fibre maturation is evident by a twisted ribbon-like structure beginning 45 to 60 dpa [2,4]. While cells are growing, cellulose is synthesised by the condensation of glucose molecules at enzyme complexes, each of which generates 36 cellulose molecules; these lie in the same direction and crystallise into long microfibrils [5]. In studies of the crystalline structures of developing cotton fibres, Paralakar [6] showed that the crystalline structure at 5 dpa belonged to cellulose I; Tuichiev et al. [7] suggested that immature cotton fibres up to 10 days after flowering showed crystalline structure cellulose III, while the cellulose I was shown only for mature fibres; Chanzy et al. [8] noted that cellulose of the primary wall of cotton at 15 dpa possesses the crystalline structure of cellulose IV; Hsieh et al. [4,9] and Hu and Hsieh [1,10] demonstrated that crystallinity increases with fibre development; Hsieh et al. [4] showed that the most significant increase in crystallinity occurs between 20 and 35 dpa, equivalent to the first two weeks of secondary cell wall synthesis or the fourth and fifth weeks of entire fibre development. It is reported that no change in crystallinity is contributed by development beyond 35 dpa [4].

There is a loss of water and the fibres dehydrate when the cotton boll starts to open and fibres become flattened and twisted. After dehydration, the cross-section of cotton fibres is kidney-shaped, however the shape is near circular in fully developed, thick-walled, mature fibres and curled in thin-walled, immature fibres [11,12]. Fibre maturity is probably the most misunderstood and least well-defined term in textile industry [13,14]; the term, fibre maturity, is used to describe the degree of development of the fibre wall [14,15]. The degree of cell wall thickening (θ) is calculated from the measured parameters of the cross-sectional area and the perimeter of the cell wall. Although determining θ is theoretically the most accurate approach of measuring fibre maturity, measurements are affected by significant experimental error because of fibre preparation and the limited number of fibres that can be

practically measured [15]. Some studies on measuring the development of cotton cell-wall thickening have been reported using different techniques: cross-section image analysis [14,16,17]; scanning probe microscopy (SPM) [11]; scanning electron microscopy (SEM) [18]; X-ray fluorescence spectroscopy (XRF) [19]; Fourier-transform infrared spectroscopy (FT-IR) [20]; and Goldthwait's method using a combination of two dyes, C.I. Direct Red 81 and C.I. Direct Green 26 [21].

Long et al. [15] measured the maturity of developing Pima (*Gossypium barbadense*) and Upland (*Gossypium hirsutum*) cotton fibres using an automated polarized light microscopy technique (SiroMat instrument). They pointed out that the fibre maturity increased as fibres developed – Upland fibres have higher average maturity, but Pima fibres matured quicker than Upland fibres. Wartelle et al. [19] studied cotton fibre maturity by X-ray fluorescence spectroscopy and Advanced Fibre Information System (AFIS) – they pointed out that these two techniques used together provide a more direct, quantitative measure of cotton maturity than other methods in use.

Abidi et al. [22] studied structural changes of developing cotton fibres using FT-IR; differences in structural evolution was reported for two cotton cultivars (*Gossypium hirsutum* L. cv. TX19 and TX55) where transition between primary and secondary cell wall occurred between 17 and 18 dpa for TX19 cultivar fibres, and between 21 and 24 dpa for fibres from TX55 cultivar. The same authors supported these findings by thermogravimetric analysis [23], and changes in sugar composition and cellulose content using HPLC [24]. Seagull et al. [25] showed significant increases in fibre diameter during the first 30 days of fibre development for 4 genotypes from two species (*Gossypium hirsutum* and *Gossypium barbadense*); all genotypes started secondary wall synthesis by 20 dpa, as indicated by significant increases in wall birefringence.

Ceylan et al. [26] studied moisture sorption in developing cotton fibres (*Gossypium hirsutum*) by dynamic vapour sorption. Two distinct stages of developing cotton fibres were reported: At the first stage from 21 to 25 dpa elongation of the fibres occurs and at the second stage above 25 dpa the secondary cell wall becomes dominant over the primary cell wall; during the first stage moisture sorption is very high in comparison to the second stage. Young fibres showed preference for polylayer water adsorption, probably due to the hygroscopic nature of the fibre components, and due to the fairly large total surface area of immature fibres. During the second stage cellulose content increases with the dpa and the maximum absorbance capacity is lower in comparison to the first stage.

Herein, the aim of this work is to analyze whether the application of novel analytical techniques such as interference polarized-light microscopy and immunofluorescence analysis using carbohydrate-binding modules (CBM), enables a better understanding of the structural properties of and crystallinity changes in developing cotton fibres. It has been previously reported that CBMs can be used to study the cell wall composition of cellulose [27, 28], and in our previous research we have demonstrated that CBMs can be successfully employed to monitor changes in crystallinity in cotton treated with different concentrations of sodium hydroxide [29]. In this work, CBMs were used to study crystallinity changes of developing cotton fibres and results were compared to both structural changes monitored using interferometric methods and also crystallinity changes measured by Attenuated Total Reflectance Fourier-transform Infrared (ATR-FTIR) spectroscopy.

2. Experimental Section

2.1. Materials

Plants from a conventional FiberMax cotton (*Gossypium hirsutum*) variety were grown in 5 L pots containing a Perlite soil mixture, in a greenhouse with 16 hours of artificial sunlight per day and maintained between 25°C and 30°C. Flowers were tagged as soon as they appeared, and harvested at the relevant dpa or days after flowering. Fibres from bolls at different developmental stages including green bolls that were 17, 20, 22, 24, 26, 35, 40, 45, 50, and 55 dpa and one boll that was matured and opened on the plant at 60 dpa were included. Bolls from 12 different plants were studied for all assays. Green and mature bolls were opened and the fibres were separated from the seeds by hand within 1 hour of harvesting. Fibres in young fruit were packed tightly together and bound by a mucilaginous matrix when dried out. To break down this matrix and to help to individualize fibres, fibres were rinsed in 70% ethanol for approximately 10 min, then left in air to dry. Carbohydrate-binding modules CBM3a and CBM17 used in this study were supplied by Prof. Harry Gilbert, Newcastle University (UK); CBM3a binds to a crystalline cellulose [30] and CBM17 binds to a non-crystalline regions of cellulose [27,31]. All other chemicals were purchased from Sigma-Aldrich.

2.2. Resin embedding and sectioning for transmission electron microscopy (TEM)

Cotton samples were fixed with 2.5% glutaraldehyde in 0.1 M phosphate buffer for 2.5 h, followed by washing two times for 30 min with 0.1 M phosphate buffer. After washing, samples were fixed overnight with 1.0% osmium tetroxide; OsO₄ was made up in the same buffer as the primary fixative. Samples were again washed two times for 30 min with 0.1 M phosphate buffer. After washing, samples were dehydrated using an ascending alcohol series

(20%, 40%, 60%, 80%, and two times 100%) for 30 min for each change. Samples were imbedded in 50/50% propylene oxide/Araldite (resin) overnight and then for several hours in 75/25% Araldite/propylene oxide. Samples were transferred to embedding moulds with fresh Araldite. Polymerisation of the resin embedded fibre was completed overnight at 60°C. Sections were cut on a Reichert Jung Ultracut Microtome to a thickness of 0.5 µm. By using FEI Spirit G2 12 BioTWIN TEM running at 120kV, micrographs of cross-sections were obtained.

2.3. Cross-sectional image analysis

Image analysis software ‘Image-Pro Plus Version 4.0’ was used to assist calculation of cross-sectional area. For each dpa, 5 cross-section images or more were analysed. Figure 1 shows an example of cotton fibre cross-section, from where the following parameters were calculated. Cross-sectional area of cotton wall (A_w) is given by Equation 1:

$$A_w = A_1 - A_2 \quad (1)$$

where A_1 is the inside/core fibre area (lumen), and A_2 is outside/total fibre area.

The degree of cell wall thickening (θ) is ratio of the cross-sectional area of the fibre wall (A_w) and the area of a circle with the same perimeter (P) (Equation 2); cotton fibre maturity ratio (M) is calculated by Equation 3; cotton fibre micronaire (Mic) represents a combined measure of cotton fineness and maturity, and is calculated by Equation 4, where T is wall thickness and P is fibre cross-sectional perimeter [32]:

$$\theta = 4\pi A_w / P^2 \quad (2)$$

$$M = \theta / 0.577 \quad (3)$$

$$\text{Mic} = 2.929 \sqrt{\left(\frac{T^2(P - \pi T)^2}{P^2} + 0.2525 \right)} - 2.352 \quad (4)$$

2.4. Interferometry

Interferometric methods are used to give information about structural properties of natural and synthetic fibres, regular and irregular fibres [33-37]. These techniques have been used to evaluate the refractive indices (n^\perp and n^\parallel) and birefringence (Δn) of fibres [34,36,37]. The double refracting polarizing interference (Pluta) microscope [38] was used for determining the fibre birefringence in this study. The Pluta microscope can be used in two different modes; the subtractive and crossed position. When the microscope is set in a subtractive mode it measures the birefringence (double refraction) directly; when it is in a crossed position, the refractive indices in the case of light polarizing parallel and perpendicular to the fibre axis is measured. In this study, the microscope was adjusted to the subtractive mode. For accurate measurements the microscope was equipped with a CCD micro-camera, PC computer, and a digital monitor. Birefringence (Δn) of fibres was calculated using the Equation 5 [33]:

$$\Delta n = \Delta F \lambda / b A \quad (5)$$

where ΔF is the measured enclosed area under the fringe shift, λ is the wavelength (550 nm) of light used, b is the inter-fringe spacing, and A is cross-sectional area of the fibre. Image-Pro Plus was used to measure A with an image analysis tool that measures the image area and arrives at an absolute value using present calibration data; an average A of five samples or more was calculated using images taken by TEM. ΔF was measured from at least 20

microinterferograms. Illustrations demonstrating the application of Equation 5 on microinterferograms for a fibre with an irregular cross-section are given in [39].

Hermans' orientation factor (f) is most commonly used to characterize the molecular orientation of polymers. Hermans derived this factor in 1946 and is a measure of the degree of molecular orientation [40], which relates optical birefringence (Δn) to segmental orientation factor (Equation 6):

$$f = \Delta n / \Delta n_0 \quad (6)$$

where Δn_0 is the maximum (intrinsic) birefringence of fibres in the perfectly oriented state; because the value of Δn_0 for cotton is not available, $\Delta n_0 = 0.055$ [39] for cellulose fibres was used in this study. Samples from the fruit younger than 17 dpa were not suitable for the analysis because fibres from these samples were still bound together.

An automated Pluta interference microscope was used for capturing and recording the microinterferograms (the fibre images) at different development times (17-60 dpa). Applied subtractive position of microscope gave the non-duplicated images for the direct measurement of the cotton fibre's birefringence (Δn). An area method [35] for determining the fibre birefringence was used due to the irregularity of cotton fibres. For precise measurements, a Fourier-transform method with a software program prepared by Sokkar et al. [37], was used to convert the original microinterferograms (Figure 2) to extracted fringe contour line (sharp white fringes) on a dark background (Figure 3). For the analysis of the final contoured-line microinterferograms of cotton fibres, Image-Pro Plus software was used to calculate the inter-fringe spacing b and the area enclosed under the fringe shift ΔF . Using Equation 5 and the non-duplicated contour line images (Figure 3), birefringence Δn for cotton fibres during development was calculated; the accuracy of measuring birefringence using Pluta interference microscope is ± 0.001 [41]. From Figure 2 and 3 it is observed that the

change and deformity in the fringe shift inside the fibre become significantly different after 24 dpa.

2.5. Attenuated Total Reflectance Fourier-Transform Infrared (ATR-FTIR) Spectroscopy

Samples were subjected to FTIR spectroscopy using a Perkin- Elmer Spectrum BX spotlight spectrophotometer with diamond ATR attachment. Scanning was conducted from 4000 to 600 cm^{-1} with 64 repetitious scans averaged for each spectrum; resolution was 4 cm^{-1} and interval scanning was 2 cm^{-1} . Prior to measurement, samples were conditioned in a standard atmosphere of $65 \pm 2\%$ relative humidity and $20 \pm 2^\circ\text{C}$ for 48 h, then held in a desiccator over P_2O_5 to maintain the same atmosphere as the FTIR measurement equipment was not located in the same place. Obtained spectra were normalized to the absorbance of the O–H in-plane deformation band at 1336 cm^{-1} due to any obtained changes in this band among all examined samples. LOI ($\alpha_{1429/893}$) and HBI ($\alpha_{3336/1336}$) were calculated as proposed by O'Connor [42] and Nada [43], respectively.

2.6. Immunofluorescence analysis using carbohydrate-binding modules (CBMs)

Using a 500 μl tube, samples were incubated in 5% milk protein/phosphate-buffered saline (PBS) for 30 min and then rinsed off once with PBS. His-tagged CBMs were added, 10 $\mu\text{g ml}^{-1}$ at 1 in 50 dilution and were incubated for at least 90 min at room temperature with shaking. After that, samples were washed three times with 5% PBS, 5 min per wash. A secondary antibody (anti-his, mouse) was added, diluted 1 in 1000 in 5% milk protein/PBS and incubated for at least 90 min. Samples were washed again three times with 5% PBS, 5 min per wash. A tertiary antibody (FITC – anti-mouse) was added, diluted 1 in 50 in 5% milk

protein/PBS and incubated for at least 90 min in the dark. Samples were washed three times with PBS, 5 min per wash. At next stage, Calcofluor (a fluorescent dye that stains all cellulose irrespective of crystallinity) was added for 5 min, $5 \mu\text{g ml}^{-1}$ at a 1 in 10 dilution. Samples were mounted in Citifluor anti-fade to prevent fluorescence fading, prior to viewing. Immunofluorescence imaging was combined with differential interference contrast imaging using an Olympus BX61 microscope equipped with differential interference contrast optics and epifluorescence irradiation. Images achieved for samples stained with Calcofluor showed a blue colour wherever cellulose was present, irrespective of crystallinity. Images achieved for samples labelled with CBMs showed a green colour: for CBM3a this is observed wherever crystalline cellulose was present; for CBM17 this is observed wherever amorphous cellulose was present. It should be noted that CBMs bind to the surface of the cotton fibres and cannot permeate the cellulose crystallites. Quantitative fluorescence imaging was completed using Image J software. CBM fluorescence micrographs were run through the software and intensity measurements were taken on regions of the fibre using a standard ellipse shape template. Three intensity measurements were taken for each micrograph for each treatment, with each treatment done in triplicate. Values were normalised between 0 and 1 through dividing the intensity values by the maximum value for each carbohydrate-binding module.

3. Results and Discussion

3.1. Fibre length measurements and cross-sectional image analysis

The primary cell wall determines the length of the cotton fibre, while the secondary cell wall determines fibre strength [44]. The summary of fibre length measurements of developing cotton fibres is presented in Figure 4, wherein it is observed that a significant increase in fibre

length up to 24 dpa; this observation is in agreement with Schubert et al. [45] who reported a rapid increase in fibre length to 27 dpa, and Benedict et al. [46] who showed an increase in fibre length of cotton fibres until 25 dpa. It is noted that the degree and timing of the observed changes may be dependent upon growing conditions and the genetic composition of the line.

Cross-sections of cotton fibres were analysed to calculate cotton maturity ratio, an important fibre quality property that is directly related to the amount of cellulose deposited during the secondary wall biosynthesis [2,20]. Figure 5 shows TEM cross-sections of cotton fibres during biosynthesis. Qualitatively, it is clear that cell-wall thickness increases with the time (dpa). Quantitatively, the average cross-sectional area of the cotton fibre wall (A_w) was calculated using Image-Pro Plus software. The relationship of wall area to time (days after flowering or dpa) is shown in Figure 6a, where it is observed that the cross-sectional area of the cotton fibres increases with fibre development, from approximately $40 \mu\text{m}^2$ at 17 dpa to $150 \mu\text{m}^2$ at maturity. Secondary wall thickening remains fairly low from 17 to 24 dpa and then the fibres begin to thicken rapidly, which is in general agreement with Schubert et al. [45] who reported rapidly thickening at 19 dpa and Ceylan et al. [26] who observed dominance of the secondary cell wall over the primary cell wall only beyond 25 dpa. Goynes et al. [48] suggested that secondary wall development starts at 15 dpa. Our results also support an overlap between secondary cell wall formation and fibre elongation, which is in line with several papers that show a considerable overlap between these two phases [26,45,46]; other references [47,49] reported that secondary cell wall thickening does not start until the elongation phase is complete. These differences between reports might be due to the insensitivity of certain methods to measure small increases in fibre wall thickness during the early phases of secondary cell wall formation or to differences between cotton genotypes. As fibres do not all develop in the same way, uneven changes in the mean degree

of cell wall thickening are observed [15], as such, the process of sectioning cotton fibres and measuring the wall area is a process fraught with experimental error [50]. Micronaire is widely used test method as an indicator of cotton fibre fineness (linear density) and maturity [32,50]. High micronaire (>5.0) usually indicates coarse fibres, which do not spin successfully into fine-count yarns, whereas low micronaire (<3.5) suggests that fibre is immature and can cause neps and dye defects. Without knowledge of perimeter or fibre maturity, low micronaire of cotton fibres could result from immature fibre or genetically fine fibre (e.g. small perimeter) [51]. Figure 6b shows micronaire of cotton fibres during biosynthesis. It is observed that micronaire is constant from 17 dpa to 24 dpa and after that it increases significantly during development until maturity, from 0.5 at 24 dpa to 6.4 at 60 dpa. These results are in an agreement with results observed from Figure 6a; if the cell wall area increases during the growth, that means the fibre is thickening and according to Equation 4, the courser fibre, the higher micronaire ($\text{Mic} \propto T$).

Maturity describes the degree of cell wall thickening relative to fibre perimeter, which is an important property that affects the textile performance of cotton fibres [15]. The mature fibre is an elongated epidermal cell of the cotton ovule with a thickened secondary wall that is mainly composed of cellulose ($> 90\%$) [52]. A mature fibre is a fibre where the cell wall thickness is twice the diameter of the fibre cell lumen [13]. Whilst fibre maturity is easy to define, its measurement is more difficult, as the test methods are limited, primarily due to the time required to make measurements, hence, testing is impractical, and measured fibre parameters are not solely related to maturity (e.g. micronaire). Maturity can also be expressed as the wall area measured directly from the microscope images of cross-sectional area. The most satisfactory expression of maturity is the maturity ratio as described by Pierce and Lord [52] that measures maturity independently of differences in intrinsic fineness. Thus, the degree of thickening is defined as ratio of the wall area to the perimeter (see Equations 2 and

3). Other ratios of cross-sectional and longitudinal geometric measurements have also been used to express maturity, however the degree of thickening (θ) remains the most used and preferred measure [50]. Figure 6c shows changes in maturity ratio of cotton fibres during their development, where it is observed that M increases as fibres develop. It has been previously reported by Long et al. [15] that maturity ratio increases with fibre development.

3.2. Optical anisotropy (birefringence) of cotton fibres

Interferometric techniques provide information of the structural properties of fibres, i.e. birefringence or optical anisotropy [36]. Birefringence is a measure of the overall molecular orientation in the fibre. Figure 7a shows birefringence of cotton fibres during development, where it is observed that birefringence increases notably from 17 dpa to 26 dpa (elongation phase) and then it levels off until the fibre become fully matured. Molecular orientation arises from parallelization of the molecular chain along the fibre axis in crystalline and amorphous regions of the fibre during elongation stage [53]. From Figure 7a, it is clearly seen that the molecular orientation/alignment occurs during the cotton elongation phase owing to the fibre stretching and after 26 dpa no more stretching is involved. It has been reported that the secondary wall thickening stage does not begin before the elongation stage is completed [3,47,49]. This is also with an agreement with results observed from Figure 6a, where thickening starts at 26 dpa, which suggests that elongation is completed by the 26 dpa, as seen in Figure 6a. The main operator that correlates the optical and structural properties of fibre is birefringence. Applying Equation 6 to experimentally obtained values of birefringence, and using the intrinsic birefringence as 0.055 [39] for cellulosic fibres, the orientation factor of developing cotton fibres is calculated (Table 1). It is observed that orientation factor also increases during development. Developing process reflects an increase

in the degree of anisotropy, which is an increase in chain orientation; therefore the orientation factor increases [54].

For correlating the structure and property of cotton fibres; the relation between birefringence and maturity ratio has been suggested. Figure 7b illustrates the birefringence changes of cotton fibres during maturation, where a remarkable increase of birefringence is observed at the lower maturity ratio values a plateau is reached at a maturity ratio of 0.3.

3.3. Attenuated Total Reflectance Fourier-Transform Infrared (ATR-FTIR) spectroscopy compared with quantitative immunofluorescence labelling with CBMs

In previous research we have demonstrated that ATR-FTIR can be successfully employed to monitor changes in crystallinity of cellulosic fibres through crystallinity indices [55,56]. Immunofluorescence labelling techniques can be employed to provide visual representation of the presence of crystalline or amorphous cellulose, by designing probes attached to carbohydrate-binding modules (CBMs) which have molecular recognition for differences in crystallinity, and we have previously used this technique to quantify crystallinity changes in cellulose I [29] and cellulose II [56] in comparison with ATR-FTIR. CBMs, with distinct molecular recognition capacities, have been used to locate in situ the presence of crystalline and amorphous regions of cellulose in plant materials [57]. However, such biological techniques have never been used to quantify molecular changes in cotton fibres during development, yet they offer a new method of qualitative and quantitative measurement of changes to the structure of cellulose that occur during the development of cotton fibres. The advantages of this technique are that no changes in crystallinity of the fibre occur during sample preparation, there is potential for increased sensitivity, and the ability to detect crystallinity changes in individual fibres, rather than the bulk of the sample in other analytical

methods. In contrast to spectroscopy, CBMs only detect crystallinity changes at the surface of the fibres.

Figures 8 and 9 show indirect immunofluorescence analysis of crystalline cellulose-directed CBM3a and amorphous cellulose-directed CBM17 binding to the surface of developing cotton fibres. Micrographs shown in Figures 8 and 9 only provide qualitative analysis and in order to provide quantitative analysis of these visualized changes in cellulose crystallinity image analysis was used to convert fluorescence signals for each treatment into relative values.

O'Connor et al. [42] the IR absorption band at 1429 cm^{-1} as typical of crystalline regions in the polymer and the absorption band at 893 cm^{-1} typical of amorphous regions; the ratio of these two bands is referred to as the “lateral order index” (LOI). LOI can be used to interpret qualitative changes in cellulose crystallinity; generally, as LOI decreases crystallinity also decreases [42,58]. Figure 10 shows indirect immunofluorescence detection of CBM3a binding to the surface of developing cotton fibres in comparison to changes in LOI from ATR-FTIR analysis. It is evident that from the comparison of LOI and CBM3a results there is a significant increase in the degree of crystallinity from 17 to 26 dpa of cotton fibres for CBM3a and until 35 dpa for LOI. This is also in agreement with birefringence results (Figure 7a). Hu and Hsieh [1] studied crystalline structure of developing cotton fibres using wide-angle X-ray scattering (WAXS) diffraction and reported that the most significant increase in the degree of crystallinity is between 21 and 34 dpa. Hsieh et al. [4] reported that crystallinity occurs between 20 and 35 dpa, and development beyond that does not contribute to any changes in crystallinity. These observations suggest that these analysis techniques could be more sensitive in detecting crystallinity changes early in fibre development than previous studies.

Hydrogen Bond Intensity (HBI) can also be used to interpret qualitative changes in crystallinity in cellulose; HBI compares the ratio of absorption bands at 3336 cm^{-1} and 1336 cm^{-1} , which is closely related to the degree of intermolecular regularity (crystallinity) [59]. Even though an increase in HBI represents an increase in hydrogen-bonding between certain hydroxyl functions in cellulose, it is generally accepted that as crystallinity of the cellulose increases, HBI decreases [43]. Figure 11 shows changes in HBI of developing cotton fibres in comparison of the quantification of amorphous cellulose-directed CBM17 binding. From obtained results the same trend of HBI and CBM17 binding is observed. HBI increases up to 24 dpa, which corresponds to the elongation stage of cotton fibre development. It is proposed that both intra- and inter-molecular hydrogen bonding occurs during this stage, which indicates that fibres contain more cellulose chains in a well ordered form leading to a higher HBI between neighbouring cellulose chains, resulting in higher crystallinity [60]. This is also in agreement with obtained results for birefringence (Figure 7a), where the most significant changes in crystallinity occur due to the drawing of the fibre. A decrease of HBI is observed from 24 to 40 dpa where it is proposed that no significant change in inter-molecular hydrogen bonds occurs, however change in intra-molecular orientation takes place. From 40 to 60 dpa, an increase in HBI is obtained, which may be explained in terms of moisture content. When water molecules bind to the hydroxyl groups in the amorphous region of the cotton fibre, hydrogen bonds are broken and the internal strain of the amorphous chain is relaxed, accordingly, molecular chains in the amorphous region rearrange to a more ordered structure [61], potentially resulting in an increase in HBI. CBMs only bind to the surface of the cotton fibres and cannot access fibre interiors, whereas the ATR-FTIR techniques are assaying throughout the fibres. It is of large interest that the binding of the crystalline cellulose-directed CBMs are particularly sensitive to changes during development. These two cellulose recognition capabilities are therefore quite distinct and do not merely appear to recognise two

different cellulose structures; these binding profiles also indicate the capacity for a range of states of cellulose structures at cotton fibre surfaces.

4. Conclusions

Developing cotton fibres were examined from days 15 to 60 after flowering during development. A significant increase in fibre length is observed to 24 dpa, which suggests that fibre elongation stops at that time. Cross-sections of cotton fibres were analysed to calculate properties of fibres and cotton maturity. It was observed that the cross-sectional area of the cotton fibres increased with fibre development, from approximately $40 \mu\text{m}^2$ at 17 dpa to $150 \mu\text{m}^2$ at maturity. Secondary wall thickening remained fairly low from 17 to 24 dpa and then the fibres began to thicken rapidly. Micronaire increased during development, it was constant from 17 dpa to 24 dpa, after which time significant change occurred until mature. These results are in an agreement with results observed from the wall area thickening – maturity ratio increased as fibres developed.

Interferometry provides information of the opto-structural properties of fibres, i.e. birefringence (Δn) and orientation factor (f). An automated Pluta interference microscope was used for capturing and recording microinterferograms of cotton fibres. Birefringence and molecular orientation of cotton fibres increased significantly from 17 dpa to 26 dpa and then achieved plateau. Molecular orientation takes place during the cotton elongation phase due to the natural stretching up to 26 dpa, which is in agreement with results observed from wall area, where thickening started at 26 dpa, suggesting that elongation is completed by 26 dpa, as shown by birefringence.

ATR-FTIR and immunofluorescence labelling techniques were used to analyse changes in crystallinity of developing cotton fibres. It was evident from the lateral order index (LOI) and CBM3a results that there was a significant increase in the degree of crystallinity from 17 dpa to 26 dpa of cotton fibres, which is also in agreement with results obtained from birefringence. Hydrogen bond intensity (HBI) increased to 24 dpa, which corresponds to the elongation stage of cotton fibre development and fibre formation. This is also in agreement with obtained results from birefringence where the most significant changes in crystallinity occurred due to natural drawing of the fibre. A decrease in HBI was observed from 24 to 40 dpa, where it is proposed that no significant change in intermolecular hydrogen bonds occurred. From 40 to 60 dpa an increase of HBI was obtained; as the presence of water molecules in amorphous regions allows molecular chains to rearrange to form a more ordered structure, corresponding to an increase in HBI.

Immunofluorescence labelling techniques offer a new method of qualitative and quantitative measurement of changes of the cellulose structure that occur during the development of cotton fibre. The advantages of the technique are that no changes in crystallinity of the fibre are caused in the sample preparation, there is potential for increased sensitivity, and also the ability to detect crystallinity changes in individual fibres, which is not readily feasibility with IR and XRD techniques. In contrast to ATR FT-IR spectroscopy, CBMs only detect crystallinity changes at the surface of the fibres.

5. Acknowledgements

The authors thank Bayer CropScience NV, Belgium for the provision of a scholarship to AK. The authors also thank The Biotechnology and Biological Sciences Research Council

(BBSRC) and Bayer CropScience NV for the provision of a BBSRC Industrial CASE Award to TASB.

6. References

1. Hu, X.-P. and Hsieh, Y.-L., Crystalline structure of developing cotton fibers. *Journal of Polymer Science Part B: Polymer Physics*, 1996. **34**(8): 1451-1459.
2. Hsieh, Y.-L., Chemical structure and properties of cotton, in *Cotton: Science and technology*, Gordon S. and Hsieh Y.-L., Editors. 2007, Woodhead Publishing Limited: Cambridge. pp. 3-34.
3. Basra, A.S. and Malik, C.P., Development of the cotton fiber, in *International review of cytology*, G.H. Bourne and J.F. Danielli, Editors. 1984, Academic press, Inc.: London. pp. 65-113.
4. Hsieh, Y.-L., Hu, X.-P., and Wang, A., Single Fiber Strength Variations of Developing Cotton Fibers-Strength and Structure of *G. hirsutum* and *G. barbedense*. *Textile Research Journal*, 2000. **70**(8): 682-690.
5. Hearle, J.W.S., Physical structure and properties of cotton, in *Cotton: Science and technology*, S. Gordon and Hsieh Y.-L. , Editors. 2007, Woodhead Publishing Limited: Cambridge. pp. 35-67.
6. Paralikar, K.M., Electron diffraction studies of cotton fibers from bolls during early stages of development. *Journal of Polymer Science Part C: Polymer Letters*, 1986. **24**(8): 419-421.
7. Tuichiev, S.T., Lavrent'ev, V.V., Kuznetsova, A.N., and Ginzburg, B.M., Cellulose structure during biosynthesis in cotton plants. *Vysokomolekulyarnye Soedineniya, Seriya B: Kratie Soobshcheniya*, 1989. **31**(11): 827-830.

8. Chanzy, H., Imada, K., and Vuong, R., Electron diffraction from the primary wall of cotton fibers. *Protoplasma*, 1978. **94**(3): 299-306.
9. Hsieh, Y.-L., Hu, X.-P., and Nguyen, A., Strength and Crystalline Structure of Developing Acala Cotton. *Textile Research Journal*, 1997. **67**(7): 529-536.
10. Hu, X.-P. and Hsieh, Y.-L., Effects of Dehydration on the Crystalline Structure and Strength of Developing Cotton Fibers. *Textile Research Journal*, 2001. **71**(3): 231-239.
11. Maxwell, J.M., Gordon, S.G., and Huson, M.G., Internal Structure of Mature and Immature Cotton Fibers Revealed by Scanning Probe Microscopy. *Textile Research Journal*, 2003. **73**(11): 1005-1012.
12. Rollins, M.L. and Tripp, V.W., Optical and Electron Microscopic Studies of Cotton Fiber Structure. *Textile Research Journal*, 1954. **24**(4): 345-357.
13. Bradow, J.M. and Davidonis, G.H., Review. Quantitation of fiber quality and the cotton production-processing interface: A physiologist's perspective. *The journal of cotton science*, 2000. **4**: 34-64.
14. Thibodeaux, D. and Rajasekaran, K., Development of new reference standards for cotton fiber maturity. *Journal of Cotton Science*, 1999. **3**(4): 188-193.
15. Long, R.L., Bange, M.P., Gordon, S.G., Constable, G.A., Measuring the Maturity of Developing Cotton Fibers using an Automated Polarized Light Microscopy Technique. *Textile Research Journal*, 2010. **80**(5): 463-471.
16. Xu, B. and Pourdeyhimi, B., Evaluating Maturity of Cotton Fibers Using Image Analysis: Definition and Algorithm. *Textile Research Journal*, 1994. **64**(6): 330-335.
17. Thibodeaux, D.P. and Evans, J.P., Cotton Fiber Maturity by Image Analysis. *Textile Research Journal*, 1986. **56**(2): 130-139.
18. Goynes, W., Microscopic Determination of Cotton Fiber Maturity. *Microscopy and Microanalysis*, 2003. **9**(SupplementS02): 1294-1295.

19. Wartelle, L.H., Bradow, J.M., Hinojosa, O., Pepperman, A.B., Sassenrath-Cole, G., and Dastor, P., Quantitative Cotton Fiber Maturity Measurements by X-ray Fluorescence Spectroscopy and Advanced Fiber Information System. *Journal of Agricultural and Food Chemistry*, 1995. **43**(5): 1219-1223.
20. Yongliang L., Thibodeaux, D., and Gamble, G., Development of Fourier transform infrared spectroscopy in direct, non-destructive, and rapid determination of cotton fiber maturity. *Textile Research Journal*, 2011. **81**(15): 1559-1567.
21. Goldthwait, C.F., Smith, H.O., and Roberts, F.T., Special Dyeing of Cotton on the Seed Gives Visual Evidence of Changes During Fiber Development. *Textile Research Journal*, 1950. **20**(2): 100-104.
22. Abidi, N., Cabrales, L., and Hequet, E., Fourier transform infrared spectroscopic approach to the study of the secondary cell wall development in cotton fiber. *Cellulose*, 2010. **17**: 309-320.
23. Abidi, N., Cabrales, L., and Hequet, E., Thermogravimetric analysis of developing cotton fibers, 2010. **498**: 27-32.
24. Abidi, N., Hequet, E., and Cabrales, L., Changes in sugar composition and cellulose content during the secondary cell wall biogenesis in cotton fibers, 2010. **17**: 153-160.
25. Seagull, R.W., Oliveri, V., Murphy, K., Binder, A., and Kothari, S., Cotton fiber growth and development 2. Changes in cell diameter and wall birefringence. *The Journal of Cotton Science*, 2000. **4**: 97-104.
26. Ceylan, O., Van Landuyt, L., Meulewaeter, F., and De Clerck, K., Moisture sorption in developing cotton fibers. *Cellulose*, 2012. **19**: 1517-1526.
27. McCartney, L., Gilbert, H.J., Bolam, D.N., Boraston, A.B., and Knox, J.P., Glycoside hydrolase carbohydrate-binding modules as molecular probes for the analysis of plant cell wall polymers. *Analytical Biochemistry*, 2004. **326**(1): 49-54.

28. McCartney, L., Blake, A.W., Flint, J., Bolam, D.N., Boraston, A.B., Gilbert, H.J., and Konx, J.P., Differential recognition of plant cell walls by microbial xylan-specific carbohydrate-binding modules. *Proceedings of the National Academy of Sciences of the United States of America*, 2006. **103**(12): 4765-4770.
29. Kljun, A., Benians, T.A.S., Goubet, F., Meulewaeter, F., Knox, J.P., Blackburn, R.S. Comparative analysis of crystallinity changes in cellulose I polymers using ATR-FTIR, X-ray diffraction, and carbohydrate-binding module (CBM) probes. *Biomacromolecules*, 2011. **12** (11): 4121-4126.
30. Boraston, A.B., Bolam, D.N., Gilbert, H.J., and Davies, G.J., Carbohydrate-binding modules: fine-tuning polysaccharide recognition. *Biochemical Journal*, 2004. **382**(3): 769.
31. Jamal, S., Nurizzo, D., Boraston, A.B., and Gideon, J.D., X-ray Crystal Structure of a Non-crystalline Cellulose-specific Carbohydrate-binding Module: CBM28. *Journal of molecular biology*, 2004. **339**(2): 253-258.
32. Montalvo, J.G., Jr, Textile technology. Relationships between micronaire, fineness, and maturity. Part I. Fundamentals. *The journal of cotton science*, 2005. **9**: 81-88.
33. Simmens, S., Birefringence determination in objects of irregular cross-sectional shape and constant weight per unit length. *Nature*, 1958. **181**: 1260-1261.
34. Hamza, A., A contribution to the study of optical properties of fibers with irregular transverse sections. *Textile Research Journal*, 1980. **50**(12): 731-734.
35. Bakarar, N. and Hamza, A., *Interferometry of fibrous materials*. 1990, Bristol: Adam Hilger.
36. Sokkar, T. and El-Bakary, M., Determination of the refractive index of fibres using the modified area method: I. Homogeneous fibres. *Optics & Laser Technology*, 2004. **36**(6): 507-513.

37. Sokkar, T., El Dessouky, H., Shams-Eldin, M., and El-Morsy, M.A., , Automatic fringe analysis of two-beam interference patterns for measurement of refractive index and birefringence profiles of fibres. *Optics and lasers in engineering*, 2007. **45**(3): 431-441.
38. Pluta, M., Interference microscopy of polymer fibres. *Journal of Microscopy*, 1972. **96**(3): 309-332.
39. Goswami, P., Blackburn, R.S., El-Dessouky, H.M., Taylor, J., and White, P., Effect of sodium hydroxide pre-treatment on the optical and structural properties of lyocell. *European Polymer Journal*, 2009. **45**(2): 455-465.
40. Hermans, P.H., Contribution to the physics of cellulose fibres. A study in sorption, density, refractive power and orientation. 1946, London: Elsevier publishing company, Inc.
41. Hamza, A., Ghander, A., and Mabrouk, M., Interferometric studies on polymer structure. *International Journal of Radiation Applications and Instrumentation. Part C. Radiation Physics and Chemistry*, 1989. **33**(3): 231-235.
42. O'Connor, R.T., DuPre, E.F., and Mitcham, D., Applications of infrared absorption spectroscopy to investigations of cotton and modified cottons. *Textile Research Journal*, 1958. **28**(5): 382-392.
43. Nada, A.-A.M.A., Kamel, S., and El-Sakhawy, M., Thermal behaviour and infrared spectroscopy of cellulose carbamates. *Polymer Degradation and Stability*, 2000. **70**(3): 347-355.
44. Xu, B. and Huang, Y, Image Analysis of Cotton Fibres Part II: Cross-sectional Measurements. *Textile Research Journal*, 2004. **74**(5): p. 409-416.
45. Schubert, A.M., Benedict, C.R., Berlin, J.D., and Kohel, R.J., Cotton Fiber Development-Kinetics of Cell Elongation and Secondary Wall Thickening¹. *Crop Science*, 1973. **13**(6): 704-709.

46. Benedict, C., Smith, R., and Kohel, R., Incorporation of ¹⁴C-Photosynthate into Developing Cotton Bolls, *Gossypium hirsutum* L. *Crop Science*, 1973. **13**(1): 88-91.
47. Hawkins, R. S., and Serviss, G. H., Development of cotton fibers in the Pima and Acala varieties. *Journal of Agricultural Research*, 1930. **40**: 1017-1029.
48. Goynes, W.R., Ingber, B.F., and Triplett, B.A., Cotton fiber secondary wall development - Time versus thickness. *Textile Research Journal*, 1995. **65**: 400-408.
49. Balls, W.L., *Studies of quality in cotton*. 1928, Macmillan and Co., Limited: London. 16-25.
50. Gordon, S., Cotton fibre quality, in *Cotton: Science and technology*, Gordon S. and Hsieh Y.-L., Editors. 2007, Woodhead Publishing Limited: Cambridge. 68-100.
51. May, O.L., Genetic variation in fibre quality, in *Cotton fibres. Developmental biology, quality improvement, and textile processing*, A.S. Basra, Editor. 1999, Food products press: Oxford. 183-229.
52. Peirce, F. and Lord, E., The fineness and maturity of cotton. *Journal of the Textile Institute Transactions*, 1939. **30**(12): 173-210.
53. Gupta, V., Melt-spinning process, in *Manufactured fibre technology*, Gupta V. and Kothari V., Editors. 1997, Chapman and Hall: London. 67-97.
54. Cai, J., Zhang, L., Zhou, J., Qi, H., Chen, H., Kondo, T., Chen, X., and Chu, B., Multifilament fibers based on dissolution of cellulose in NaOH/urea aqueous solution: structure and properties. *Advanced Materials*, 2007. **19**(6): 821-825.
55. Široký, J., Blackburn, R.S., Bechtold, T., Taylor, J., White, P. Attenuated Total Reflectance Fourier-Transform Infrared spectroscopy analysis of crystallinity changes in lyocell following continuous treatment with sodium hydroxide. *Cellulose*, 2010. **17**(1): 103-115.

56. Široký, J., Benians, T.A.S., Russell, S.J., Bechtold, T., Knox, J.P., Blackburn, R.S. Analysis of crystallinity changes in cellulose II polymers using carbohydrate-binding modules. *Carbohydrate Polymers*, 2012. **89**: 213-221.
57. Blake, A.W., McCartney, L., Flint, J.E., Bolam, D.N., Alisdair, B.B., Gilbert, H.J., and Knox, J.P., Understanding the Biological Rationale for the Diversity of Cellulose-directed Carbohydrate-binding Modules in Prokaryotic Enzymes. *Journal of Biological Chemistry*, 2006. **281**(39): 29321-29329.
58. Hurtubise, F.G. and Krassig, H., Classification of fine structural characteristics in cellulose by infrared spectroscopy - use of potassium bromide pellet technique. *Analytical Chemistry*, 1960. **32**(2): 177-181.
59. Oh, S.Y., Yoo, D.I., Shin, Y., Kim, H.C., Chung, Y.S., Park, W.H., and Youk, J.H., Crystalline structure analysis of cellulose treated with sodium hydroxide and carbon dioxide by means of X-ray diffraction and FTIR spectroscopy. *Carbohydrate Research*, 2005. **340**(15): 2376-2391.
60. Poletto, M., Pistor, V., Santana, R.M.C., and Zattera, A.J., Materials produced from plant biomass: part II: evaluation of crystallinity and degradation kinetics of cellulose. *Materials Research*, 2012. **15**(3): 421-427.
61. Hatakeyama, T., Structure and properties of the amorphous region of cellulose, In *Cellulose. Structural and functional aspects*, Kennedy J.F., Phillips G.O., and Williams P.A., Editors. 1989, Ellis Horwood Limited: Chichester. 45-52.

Figures and Tables

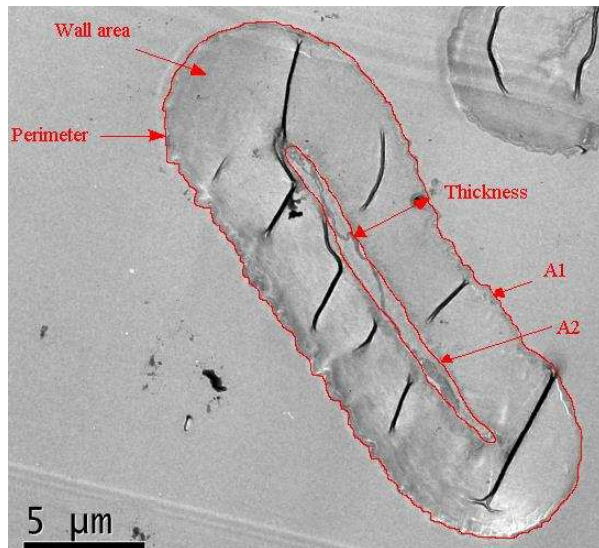


Figure 1: An example of a cotton fibre cross-section analysis using Image-Pro Plus analysis of a TEM image.

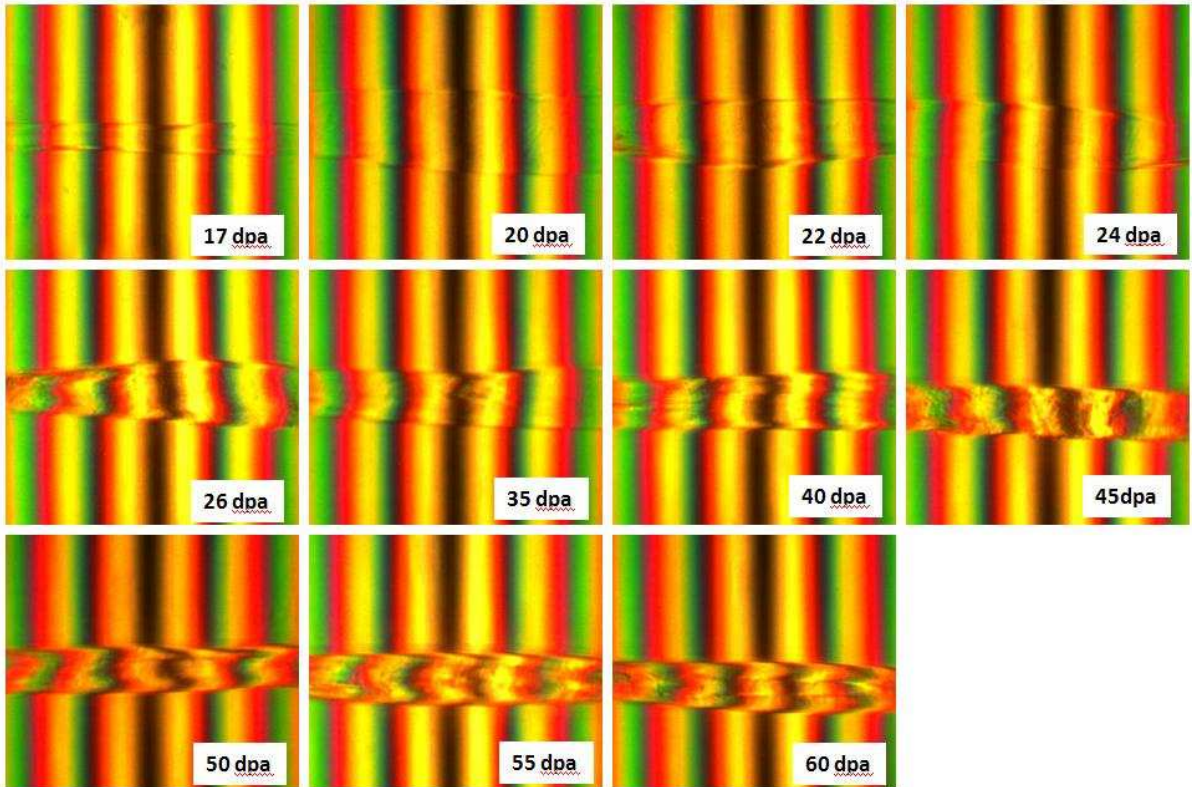


Figure 2: Microinterferograms of cotton fibres with increasing dpa. Wavelength of $\lambda = 550$ nm, taken by Pluta microscope.

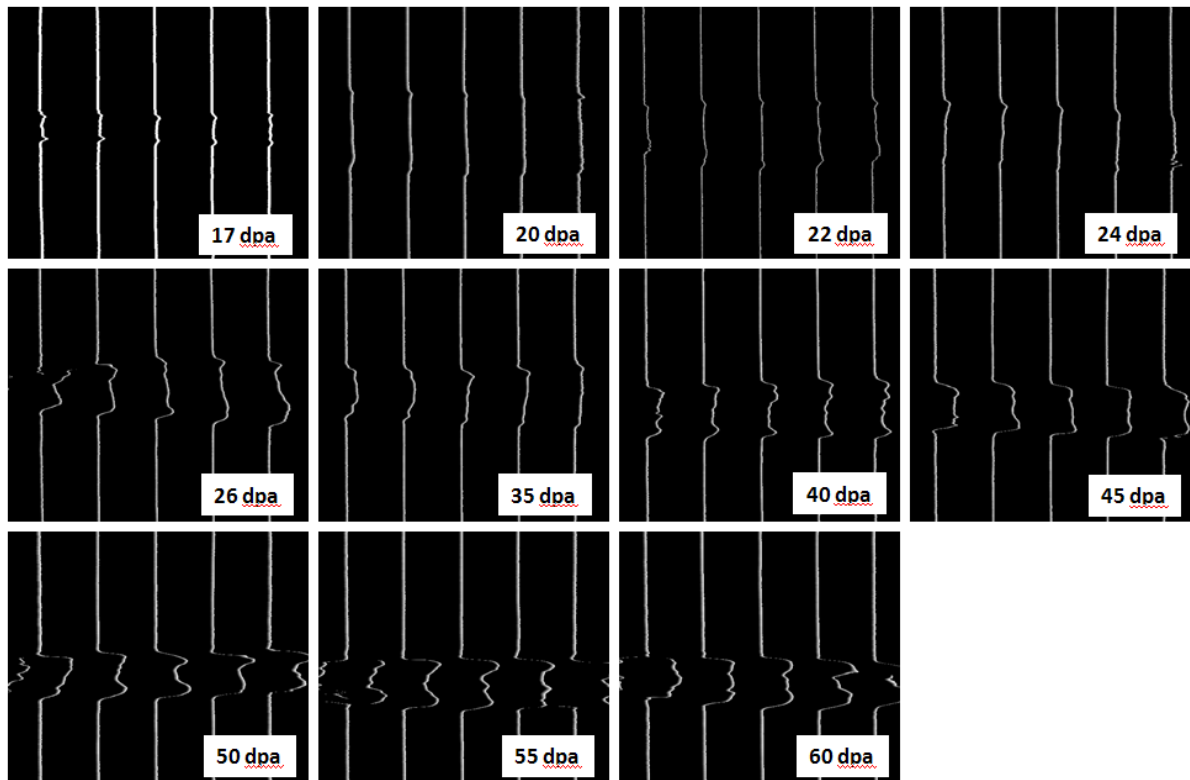


Figure 3: Microinterferograms of cotton fibres with increasing dpa from Figure 2 with extracted fringe contour line on a dark background.

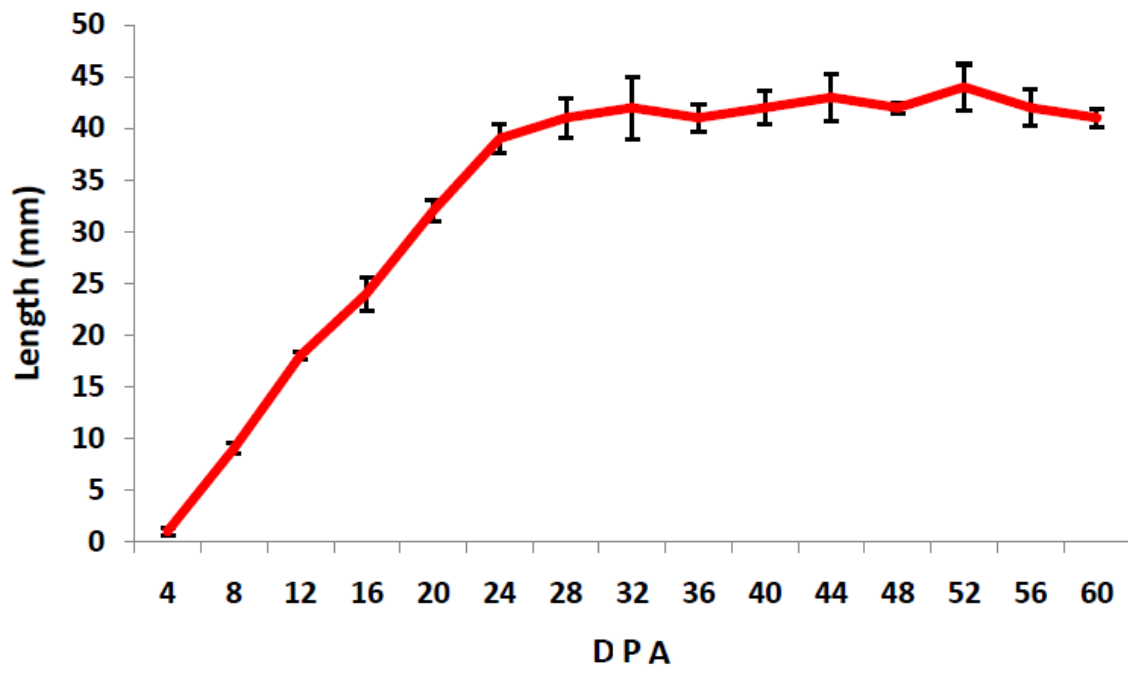


Figure 4: Length of developing conventional FiberMax cotton fibres with increasing dpa. Error bars are based on calculated standard deviation.

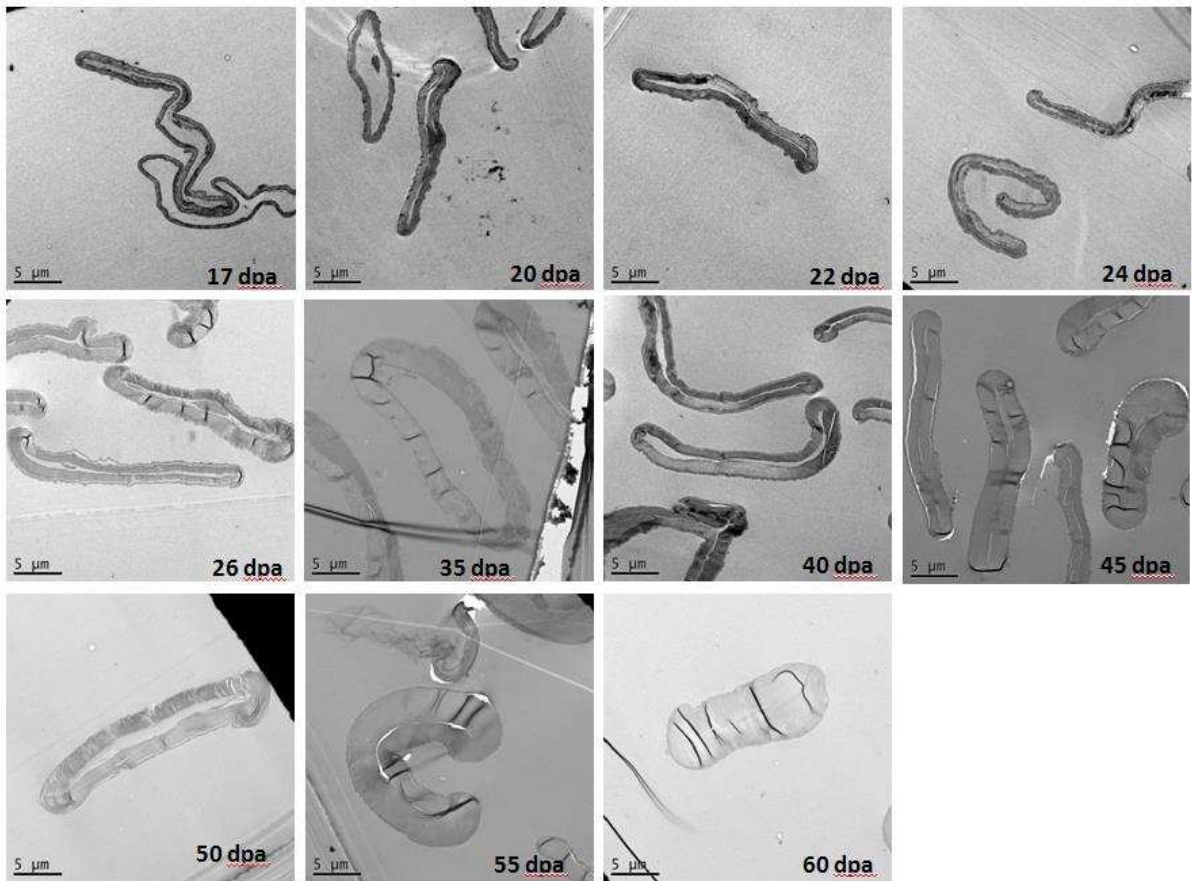


Figure 5: TEM transverse-sections of conventional FiberMax cotton fibres with increasing dpa during development.

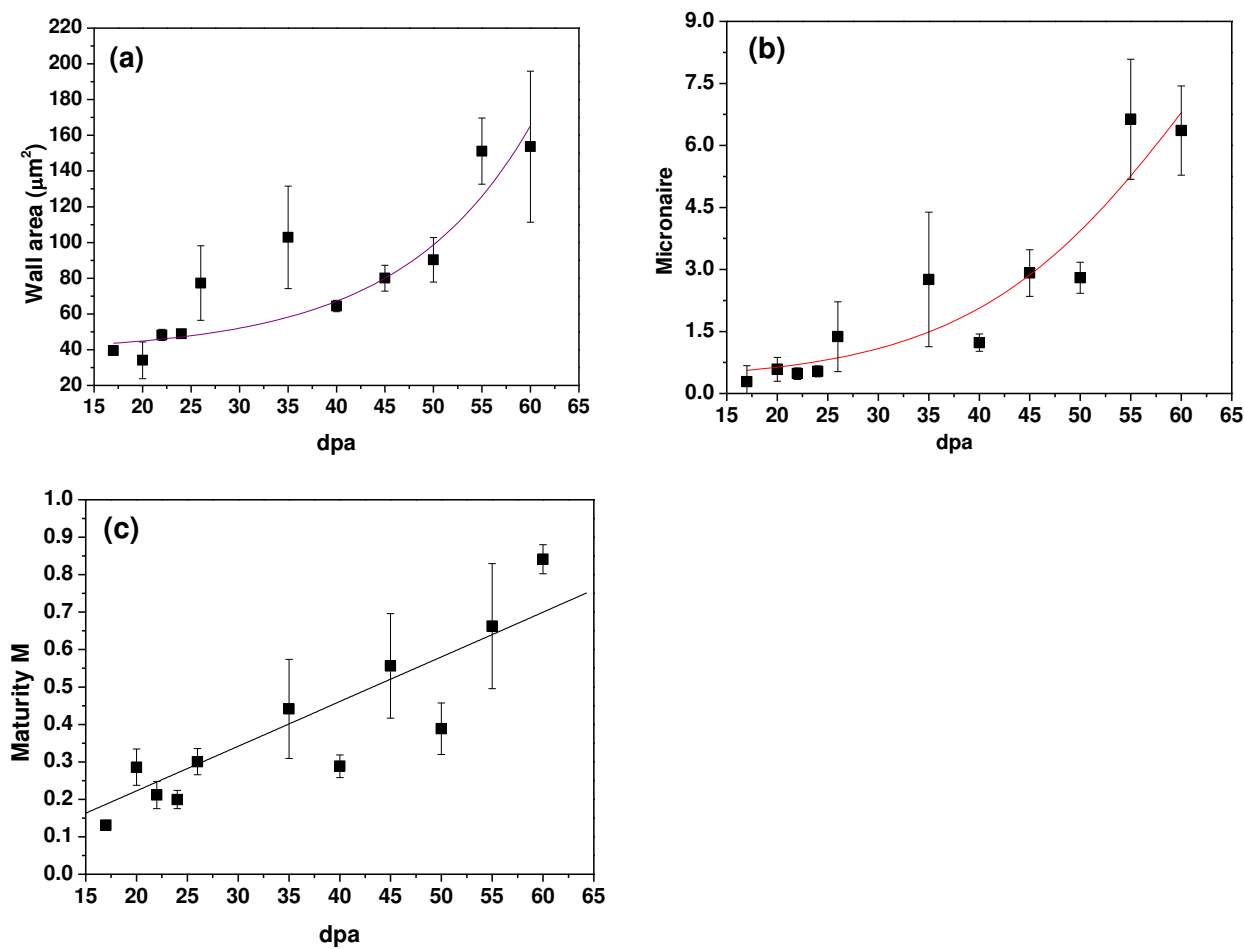


Figure 6: Analysis of conventional FiberMax cotton fibre properties with increasing dpa during development: (a) cross-sectional area, (b) micronaire, and (c) maturity. Error bars are based on calculated standard deviation.

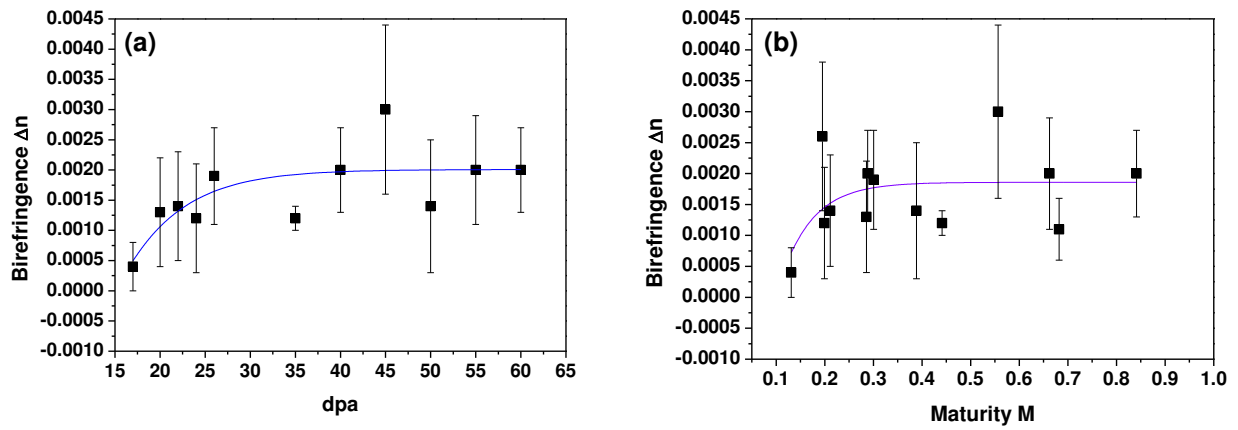


Figure 7: Birefringence (Δn) of conventional FiberMax cotton fibres: (a) with increasing development time (dpa); and (b) during maturation (M). Error bars are based on calculated standard deviation.

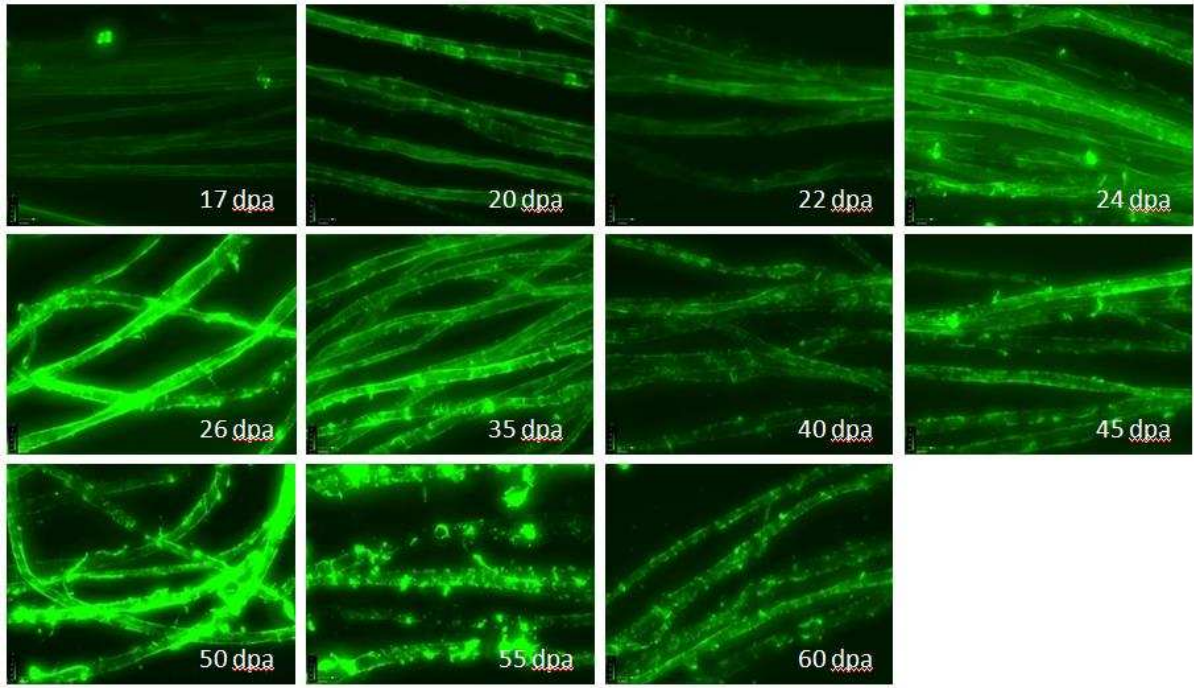


Figure 8: In situ fluorescence imaging of the binding of crystalline cellulose-directed CBM3a to developing conventional FiberMax cotton fibres, with increasing dpa.

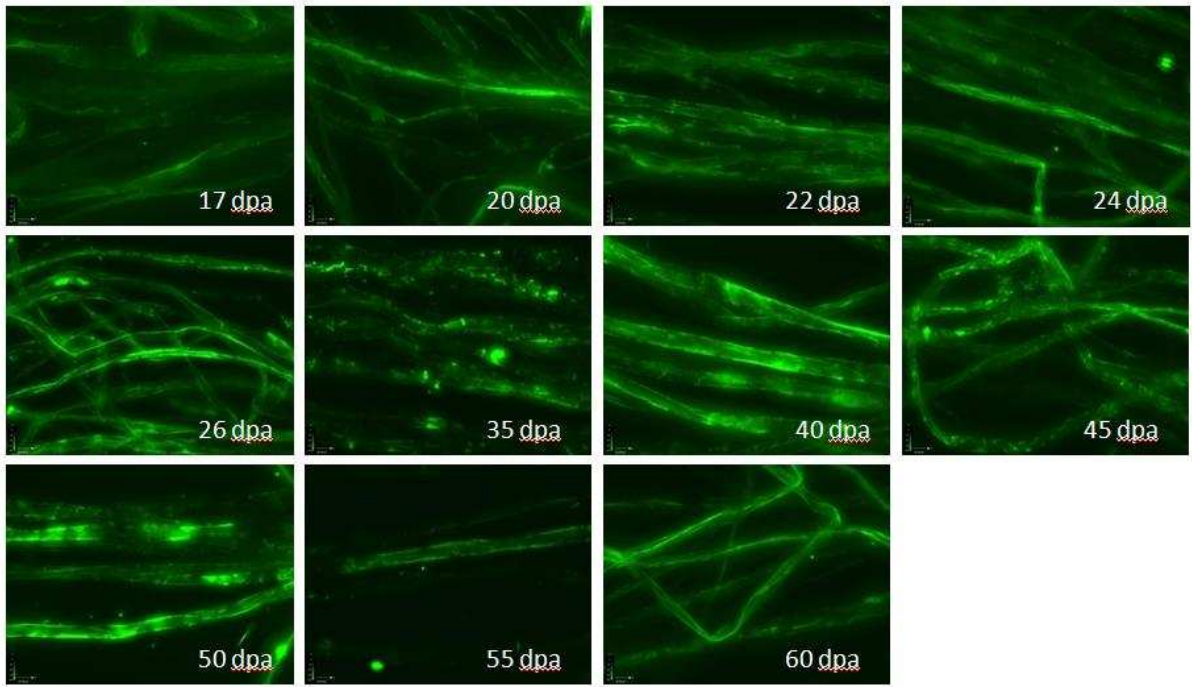


Figure 9: In situ fluorescence imaging of the binding of amorphous cellulose-directed CBM17 to developing conventional FiberMax cotton fibres, with increasing dpa.

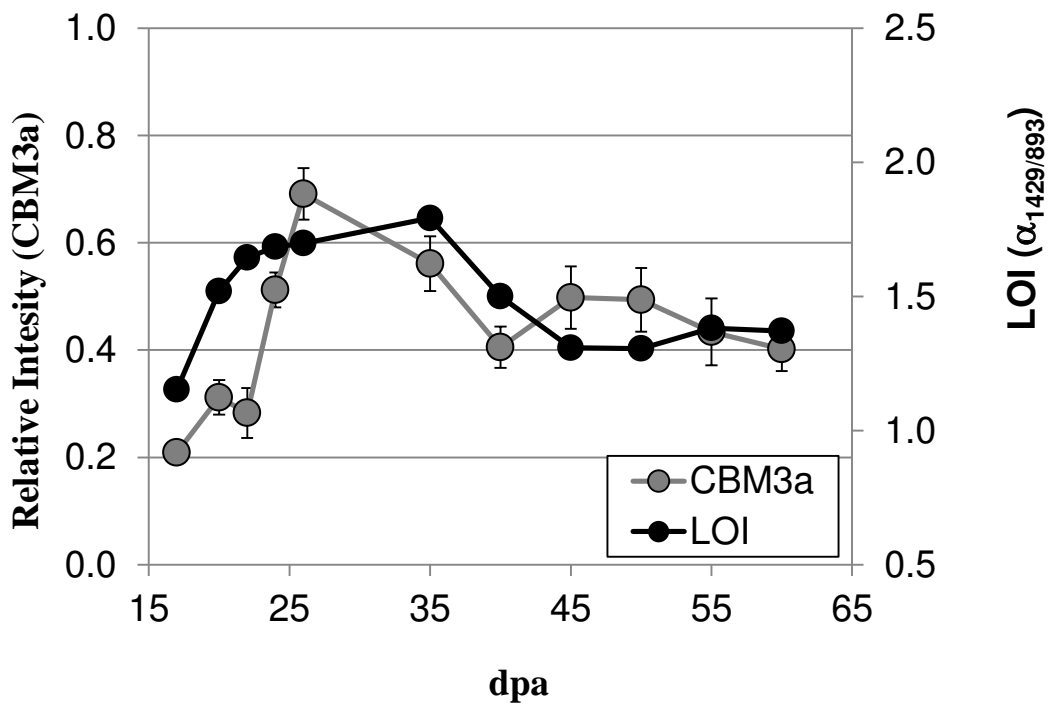


Figure 10: Analysis of binding of crystalline cellulose-directed CBM3a to developing conventional FiberMax cotton fibres in comparison with LOI (ATR-FTIR), with increasing dpa. Error bars are based on calculated standard deviation.

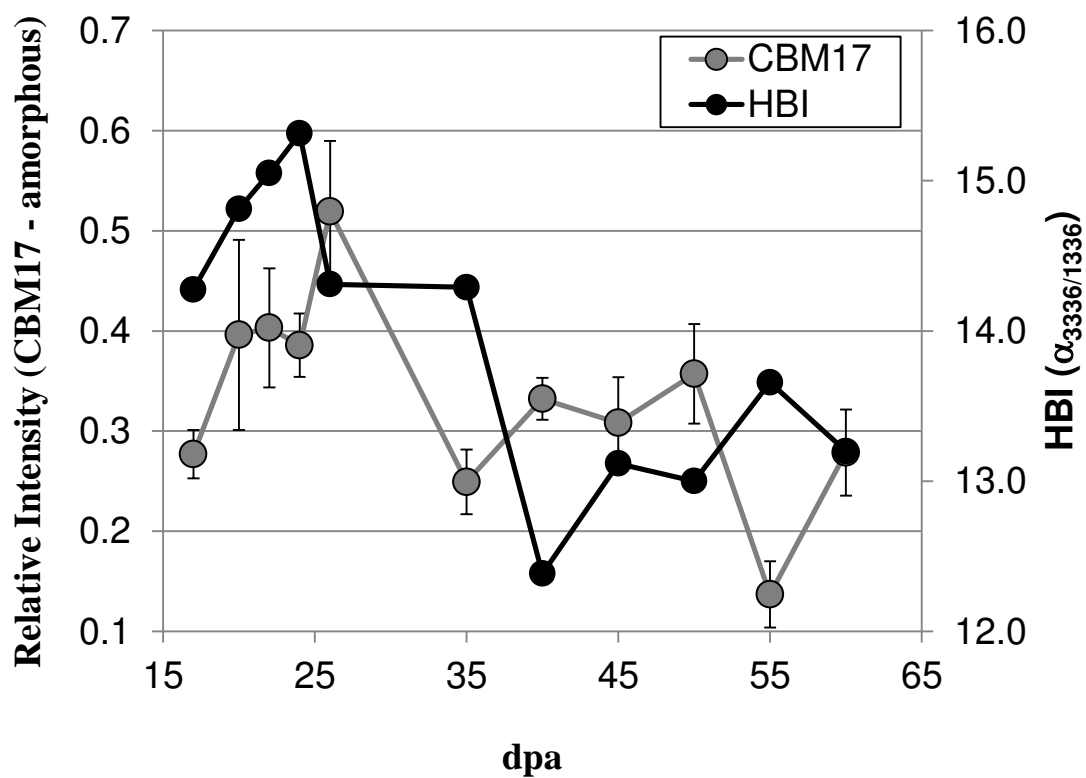


Figure 11: Analysis of binding of amorphous cellulose-directed CBM17 binding to developing conventional FiberMax cotton fibres in comparison with HBI (ATR-FTIR), with increasing dpa. Error bars are based on calculated standard deviation.

Table 1: Overall molecular orientation (f) of conventional FiberMax cotton fibres with increasing dpa.

dpa	f
17	0.007
20	0.024
22	0.025
24	0.022
26	0.035
35	0.022
40	0.036
45	0.055
50	0.026
55	0.036
60	0.036